

RESEARCH ARTICLE

Preparation and characterization of tea leaf exosome-like nanoparticles (ELNs) and its protective effect on the skin senescence in mice

Bing Li^{1,†}, Shengqiang Li^{1,†}, Yimeng Ge^{1,†}, Xueqing Wang², Jun Li², Huili Xia², Feng Guan¹, Longhua Zhu¹, Jian Ge^{1,*}

¹College of Life Sciences, China Jiliang University, Hangzhou, Zhejiang, China. ²Taizhou Food and Drug Inspection and Research institute, Taizhou, Zhejiang, China.

Received: February 11, 2025; accepted: May 25, 2025.

With improvements in quality of life and advancements in biotechnology, there is growing public interest in skin protection, particularly in delaying skin aging. Consequently, research on the mechanisms of aging and anti-aging strategies has become a major focus. In this study, exosome-like nanoparticles (ELNs) were extracted and purified from fresh leaves of West Lake Longjing green tea, characterized, and evaluated for their protective effects against skin aging using a D-galactose-induced aging model in KM mice. The results showed that the ELNs exhibited a spherical morphology with particle sizes ranging from 50 to 120 nm and a ζ -potential of -16.5 ± 0.61 mV. The ELNs contained certain lipid components and remained relatively stable under simulated physiological conditions. Following ELNs injection, skin aging in mice was significantly alleviated, accompanied by enhanced activities of superoxide dismutase (SOD) and glutathione peroxidase (GSH-Px) and a reduction in malondialdehyde (MDA) levels in skin tissues. In addition, the expression levels of MMP-1, P16, and P53 genes in mouse skin were significantly reduced, indicating that ELNs exerted a marked protective effect against skin aging in mice, which might be associated with the modulation of MMP-1, P16, and P53 expression. This study elucidated the molecular mechanisms by which ELNs delayed skin aging and offered a promising strategy for the development of natural anti-aging agents.

Keywords: tea leaves; exosome-like nanoparticles (ELNs); anti-senescence of skin; antioxidant.

*Corresponding author: Jian Ge, College of Life Sciences, China Jiliang University, 258 Xueyuan Street, Xiasha Higher Education Zone, Hangzhou 310018, Zhejiang, China. Email: gejian@cjlj.edu.cn.

[†]These authors contributed equally to this work.

Introduction

Skin senescence is a critical component of overall aging, which not only affects appearance but also contributes to various skin disorders through gradual structural and functional changes [1]. The appearance of sagging skin, wrinkles, and age spots signals the onset of skin aging, potentially leading to psychological and social issues.

Consequently, preventing and delaying skin aging has become a focal point in aesthetic medicine. Skin aging is mainly caused by natural factors (extrinsic aging) and non-natural factors (intrinsic aging), and its mechanism is still unclear. Dermal fibroblasts, the key effector cells in the aging process, are the main source of collagen secretion and play a vital role in maintaining the normal structure and physiological function of

the skin [2].

In recent years, plant-derived extracts such as lycopene (LYC) [3], ginsenosides [4], *Lycium barbarum* polysaccharides [5], and tea polyphenols [6] have been utilized to delay skin aging. However, these anti-aging compounds are prone to oxidative degradation, limiting their long-term protective effects. In addition to natural compounds, enzymatic antioxidants such as superoxide dismutase (SOD), catalase (CAT), glutathione peroxidase (GSH-PX), and peroxidase (POD) have also been employed to achieve anti-aging and antioxidant effects [7]. Nevertheless, both natural compounds and macromolecular enzymes suffer from poor skin permeability and limited stability. To enhance drug bioavailability, delivery systems such as liposomes [8] and nanocarriers [9] are often used. However, these carriers are often associated with high development costs, low encapsulation efficiency, and limited application scope.

Extracellular vesicles (EVs) are critical structures for maintaining normal physiological functions and are classified into ectosomes and exosomes based on their biogenesis and release mechanisms [10]. Plant-derived extracellular vesicles, also referred to as exosome-like nanoparticles (ELNs), are typically composed of lipids, proteins, nucleic acids, and various small bioactive molecules [11]. These ELNs exhibit tea cup-like or cup-shaped vesicles morphologies with unique membrane structures and a particle size ranging from 30 to 200 nm [12]. Numerous studies have demonstrated that ELNs can be internalized into mammalian cells *via* cytophagy, clathrin-mediated endocytosis, caveolae-mediated endocytosis, and micropinocytosis [13]. Due to their ease of uptake, ELNs are capable of efficiently delivering proteins, lipids, RNAs, and other bioactive substances into cells, thereby exerting a variety of therapeutic effects. Previous research reported that Iris-derived ELNs demonstrated to be absorbed by human keratinocytes to exert anti-aging effects [14]. Another report suggested that tea water extract provided benefits of anti-aging, anti-Alzheimer's

disease, and anti-oxidation [15]. Further, Ke *et al.* found that green tea hot water extracts had been shown to improve healthspan by enhancing stress resistance and reducing reactive oxygen species (ROS) accumulation [16]. Moreover, tea extracts have been widely used in the field of anti-aging cosmetics for years. However, the potential effects of tea-derived exosomes remain largely unexplored. Our previous research revealed that a combination of green tea-derived ELNs and LYC significantly enhanced the activity of antioxidant enzymes in fibroblasts and delayed their senescence [17].

Despite the benefits, most previous studies administered ELNs *via* oral routes, which suffered from poor absorption. This research aimed to expand the potential routes of ELNs administration by injecting ELNs directly into the dermis of mice to increase ELNs retention in the skin. This approach enabled further exploration of ELNs anti-aging mechanisms and provided a theoretical and technical foundation for the development of medical cosmetology and anti-aging products.

Materials and methods

Preparation and characterization of ELNs from tea leaves

Fresh leaves of West Lake Longjing green tea were provided by Zhejiang Shuangye Industrial Co., Ltd. (Hangzhou, Zhejiang, China). The preparation of ELNs was performed with reference to previously reported methods [18]. Fresh leaves were washed thoroughly with water and homogenized using a juicer at a leaf-to-water ratio of 1:4 (g/mL). The tea leaves juice was sequentially centrifuged at 1,000 g for 10 min, 3,000 g for 30 min, and 10,000 g for 60 min at 4°C to remove impurities. The supernatant was then subjected to ultracentrifugation at 100,000 g for 2 h at 4°C, and the pellet was resuspended in phosphate buffered saline (PBS) to obtain a crude ELN suspension. For further purification, the discontinuous sucrose density gradients of 5%, 10%, 30%, 45%, and 60% were employed. The

sample was ultracentrifuged at 200,000 g for 2 h at 4°C, and ELNs in the 30/45% layer was collected, resuspended in PBS and centrifuged at 100,000 g for 70 min to obtain purified ELNs. Morphological analysis of ELNs was conducted using Hitachi HT7700 transmission electron microscopy (Hitachi, Tokyo, Japan). The particle size and zeta potential of ELNs were evaluated by Zetasizer Nano-ZS 90 Dynamic Light Scattering System (Malvern Panaco, Almelo, Netherlands) [19]. The lipid composition of ELNs was analyzed using ultra-performance liquid chromatography - time-of-flight mass spectrometry (UPLC-TOF-MS) methods with SYNAPT G2-Si Mass Spectrometry and ACQUITY Premier HSS T3 column (Waters, Milford, MA, USA).

Experimental animals

Healthy male KM mice, SPF-grade, 8 weeks old, weighing 20 ± 2 g, were provided by Shanghai SLAC Laboratory Animal Co (Shanghai, China). The mice were housed under controlled conditions with relative humidity of $55 \pm 10\%$, temperature of 23 - 25 °C, and 12 h light-dark cycle. All animals had free access to food and water. Before starting the experiment, the mice were fed at least one week to acclimatize the aforementioned environment. The protocols and operations of this research were approved by the Experimental Animal Ethics Committee of China Jiliang University, Hangzhou, Zhejiang, China (Approval No. 2024-003).

Animal treatments

The dosages of fresh tea leaf ELNs and lycopene (LYC), as well as the method of D-gal (Sigma-Aldrich, St. Louis, MO, USA) induced modeling were referred to the previous studies with slightly modifications [20, 21]. KM mice were randomly divided into five groups, including the normal group, the model group, the ELNs group, the LYC group, and the ELNs + LYC group with 10 mice in each group. Mice in the normal group were intraperitoneally injected with 0.1 mL of normal saline every morning, while the other four groups received the same volume of D-galactose (1,000 mg/kg) daily. In the afternoon, the normal and model groups were injected with

0.1 mL of saline. The ELNs group received 2 mg/kg of ELNs, while the LYC group received 10 mg/kg of LYC, and the ELNs + LYC group received a combination of ELNs and LYC (1 mg/kg ELNs and 5 mg/kg LYC), all administered in equal volumes. The mice were executed after 42 days of treatments. The mice skin samples were either snap-frozen in liquid nitrogen or immediately fixed in 4% (w/v) formalin solution for further analysis.

HE and Sirius red staining

Mice skin tissues fixed with 4% paraformaldehyde were subjected to dehydration, de-alcoholization, paraffin embedding, sectioning, and hematoxylin staining. Sections were then immersed in 1% hydrochloric acid ethanol, rinsed with ultrapure water, counterstained with eosin, dehydrated, sealed, and observed under the microscope. For sirius red staining, skin tissue sections were stained with hematoxylin solution for 5 - 10 minutes, washed, stained with sirius red staining solution for 1 hour before rinsed with running water, dehydrated and transparent, sealed with neutral gum, and then observed under the microscope.

Measurement of skin water content and related biochemical indicators

The water content in mouse skin was ascertained by the usage of the constant temperature drying method, which involved weighing the mouse skin at a wet weight of 0.5 g, drying at 80°C for 12 hours in an oven, and weighing the dry weight. The skin moisture content was determined as follows.

$$\text{Water content} = (m1 - m2) / m1 \times 100\%$$

where m1 and m2 were the wet weight and dry weight of the skin, respectively. The hydroxyproline (HYP) and type III collagen were determined using commercial assay kits (Nanjing Jiancheng Bioengineering Institute, Nanjing, Jiangsu, China) according to the manufacturer's instructions. The malondialdehyde (MDA) content, SOD, and GSH-px activity were also

determined using the related kits (Nanjing Jiancheng Bioengineering Institute, Nanjing, Jiangsu, China).

Reverse transcription-quantitative polymerase chain reaction (RT-qPCR) analysis

The mRNA and protein expression levels of skin aging-related genes in different treatment groups were analyzed using quantitative real-time PCR (qPCR) and Western blotting. Total RNA was extracted from homogenized skin samples using the TRIzol® Plus RNA Purification Kit (Thermo Fisher Scientific, Waltham, MA, USA) and the RNase-Free DNase Set (Qiagen, Hilden, Germany). Subsequently, RNA was reverse-transcribed into cDNA using the SuperScript™ III First-Strand Synthesis SuperMix (Thermo Fisher Scientific, Waltham, MA, USA). Quantitative PCR primers were designed using Primer Premier 6.0 (<https://primer-premier.software.informer.com/6.0/>) and Beacon Designer 7.8 (<https://beacon-designer.software.informer.com/7.8/>), which included GAPDH forward primer (5'-GAA GGT CGG TGA AGG ATT TG-3') and reverse primer (5'-CAT GTA GAC CAT GTA GTT GAG GTC A-3'), MMP-1 forward primer (5'-GGG CTG TTC AAG AGC AGA GTG-3') and reverse primer (5'-CAT TGC TAG GGA AGC CAA AGA AAC T-3'), P16 forward primer (5'-CTA CGG TGC AGA TTC GAA CTG-3') and reverse primer (5'-AGC GTG TCC AGG AAG CCT T-3'), P53 forward primer (5'-GCC GAC CTA TCC TTA CCA TCA-3') and reverse primer (5'-CAG GCA CAA ACA CGA ACC TCA A-3'). qRT-PCR was conducted by utilizing the Power SYBR® Green PCR Master Mix kit (Applied Biosystems, Waltham, MA, USA). The reaction conditions were 95°C for 1 minute followed by 40 cycles of 15 seconds at 95°C, 25 seconds at 63°C. Sample Ct values were obtained from the melting point curves, and each sample was repeated three times. The relative expression levels of each gene were statistically analyzed using the formula $2^{-\Delta\Delta Ct}$.

Western blot analysis

Proteins were extracted from skin tissue homogenates and quantified using a BCA protein assay kit (Nanjing Jiancheng Bioengineering Institute, Nanjing, Jiangsu, China). The expression

levels of p16 and MMP-1 proteins were analyzed by Western blotting. Primary antibodies p16/CDKN2A (dilution ratio of 1:500) and MMP-1 (dilution ratio of 1:2,000) were purchased from Abcam (Cambridge, United Kingdom), and secondary antibodies of goat anti-mouse (H + L) (dilution ratio of 1:5,000) and goat anti-rabbit (H + L) (dilution ratio of 1:5,000) were obtained from Thermo Pierce (Thermo Fisher Scientific, Waltham, MA, USA).

Statistical analysis

All data were expressed as the mean \pm SD of at least three independent experiments and were analyzed by one-way ANOVA with Tukey's post hoc test using GraphPad Prism 9.5 software (GraphPad, San Diego, CA, USA). *P* value less than 0.05 was defined as a statistically significant difference.

Results and discussion

Structural characterization of ELNs

The ELNs isolated from fresh tea leaves showed a tea-shaped (Figure 1A) with particle sizes ranging from 50 to 120 nm (Figure 1B) and a ζ potential of -16.5 ± 0.61 mV. ELNs derived from plant sources exhibited slightly larger particle sizes compared to exosomes originating from animal cells with notable size variations observed among different plant sources [22]. The major lipid components of fresh tea leaf ELNs included 20.72% diacylglycerol (DG), 13.10% phosphatidylcholine (PC), 20.27% free fatty acids (FA), and 12.32% phosphatidylinositol (PI) (Figures 1C and 1D). The particle size distributions of tea leaf ELNs in PBS solution, simulated gastric fluid, and simulated intestinal fluid were 198.7 ± 2.92 nm, 213.1 ± 18.75 nm, and 203.7 ± 2.79 nm, respectively (Figure 1E), and the differences in the particle size distributions were not significant, which indicated that the tea leaf ELNs were more stable in gastrointestinal simulated fluid. This result provided strong evidence that fresh tea leaf ELNs could exist and function in the gastrointestinal tract.

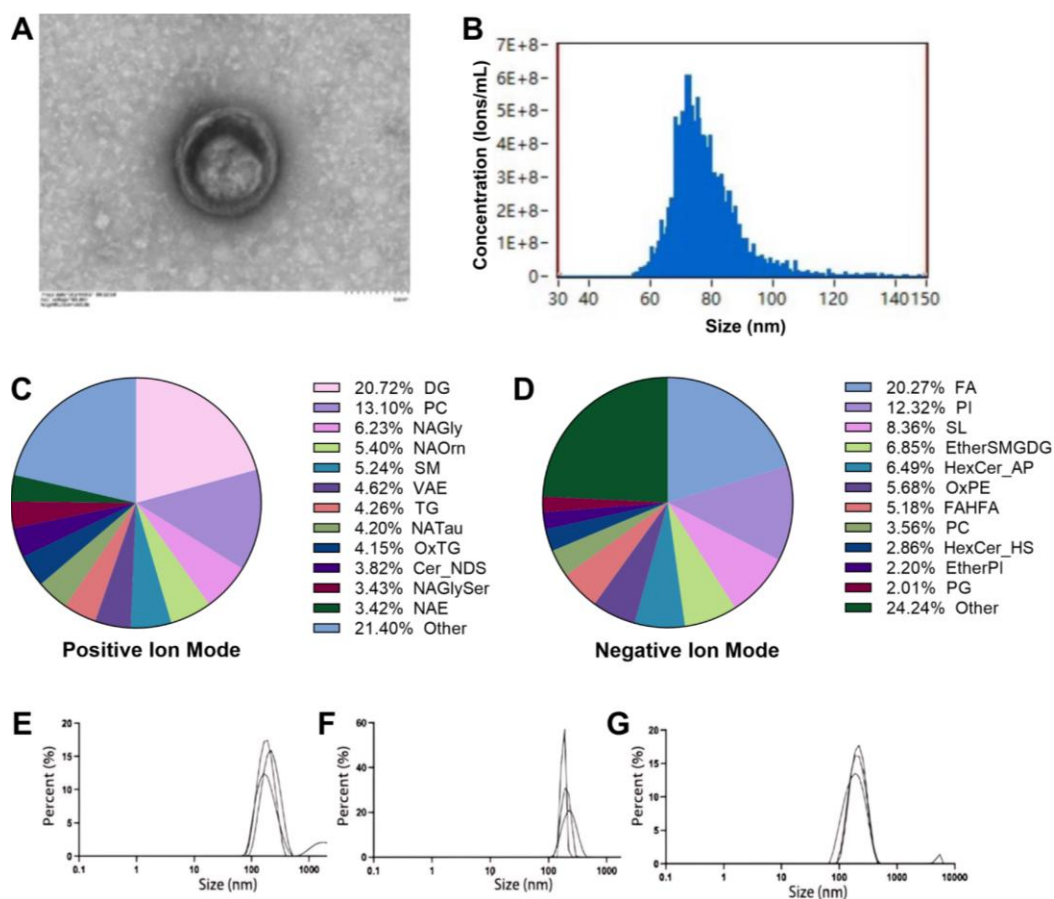


Figure 1. Characterization of ELNs by different physical and chemical analysis techniques. Morphology (A) and particle size (B) of fresh tea leaf ELNs. Lipid distribution in ELNs of fresh tea leaves in positive (C) and negative (D) ion modes. Particle size distribution of fresh tea leaf ELNs in PBS (E), simulated gastric fluid (F), and intestinal fluid (G).

Improvement of skin condition in mice

In the normal control group, the epidermis of the mouse skin remained intact with only occasional mild erythema observed. In contrast, the skin of the model group exhibited typical pathological features of aging including wrinkles, persistent erythema, and epidermal thinning. The LYC group showed some signs of erythema. However, the ELNs group and the ELNs + LYC combination group displayed smooth and healthy skin with no apparent erythema. These findings indicated that lycopene and freshly extracted tea leaf ELNs might contribute to improving skin barrier function and maintaining skin homeostasis.

Influence on the structure of mice skin tissue

The results of HE staining of skin tissue showed that, in the normal control group, the epidermis

was intact. The dermis was tightly connected to the epidermis and appeared thick with well-organized sebaceous glands and hair follicles, showing intact structures and normal morphology. Collagen fibers in the dermis were densely distributed. In contrast, the model group exhibited atrophic stratum corneum, thinned dermis, indistinct and irregularly shaped hair follicle cells, condensed and aggregated nuclei, disordered cell arrangement, and loosely organized dermal collagen fibers. In the ELNs group, dermal thickening and significant morphological restoration of skin tissues were observed. Compared to the model group, the ELNs + LYC group showed remarkably improvements including better epidermal structure, intact skin tissue, significantly thickened dermis, normal structure and

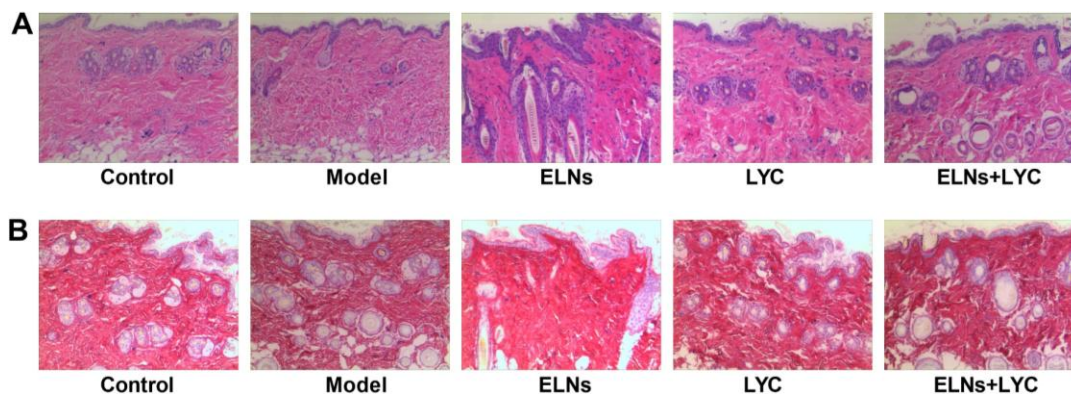


Figure 2. Structure of mice skin in different groups. **A.** HE staining. **B.** Sirius red staining.

morphology of hair follicle cells, and well-organized collagen-rich dermis (Figure 2A). The model group exhibited the lowest levels of both type I and type III collagen fibers compared to the other groups. Upon ELNs treatment, type I collagen fibers appeared densely arranged, and the amount of type III collagen fibers was greater than that in the LYC group. The ELNs + LYC group showed the highest level of type III collagen fibers among all groups (Figure 2B).

Combination of ELNs and LYC increased skin water content in mice

Both endogenous and exogenous factors can reduce skin water content, and decreased water content is a hallmark of aged skin. Therefore, skin water content serves as a critical indicator of skin aging. The results showed that D-gal treatment reduced skin water content in the model group compared to the normal group, although the difference was not statistically significant. ELNs treatment significantly increased skin water content compared to the model group ($P < 0.05$). Notably, the ELNs + LYC group demonstrated significantly higher skin water content than both the model and normal groups ($P < 0.001$) and the LYC group ($P < 0.05$) (Figure 3A).

Combination of ELNs and LYC regulated collagen metabolism in mice

Hydroxyproline (HYP), which accounts for approximately 13% of collagen, serves as an indicator of collagen metabolism [23]. The suppleness and firmness of the skin largely

depend on collagen content, and a reduction in collagen is closely associated with skin aging. HYP levels in the ELNs group were higher than those in the model group. Notably, co-administration of ELNs and LYC resulted in a more pronounced increase in HYP levels ($P < 0.05$) (Figure 3B). Type III collagen (Col3) is essential for maintaining skin elasticity and replenishing collagen levels in the skin with its content inversely correlated with age [24]. To assess the degree of skin aging in each group, Col3 levels in skin homogenates were measured and showed that Col3 content was elevated in the ELNs group compared to both the normal and model groups. Furthermore, the ELNs + LYC group exhibited significantly higher Col3 content than the model group ($P < 0.05$) (Figure 3C). D-gal-induced ROS production can lead to lipid peroxidation of fibroblast membranes, resulting in fibroblast degeneration and a reduction in dermal collagen content. It is speculated that the combination of ELNs and LYC inhibits ROS accumulation in fibroblasts, prevents membrane lipid peroxidation and cellular degeneration, and ultimately enhances Col3 levels. Therefore, co-treatment with ELNs and LYC might increase Col3 content in the skin and delay D-gal-induced skin aging.

Combination of ELNs and LYC alleviated oxidative stress in mice

oxidative stress and the overproduction of reactive oxygen species (ROS) play an important role in the skin aging process [25]. Skin aging is closely associated with oxidative stress. During

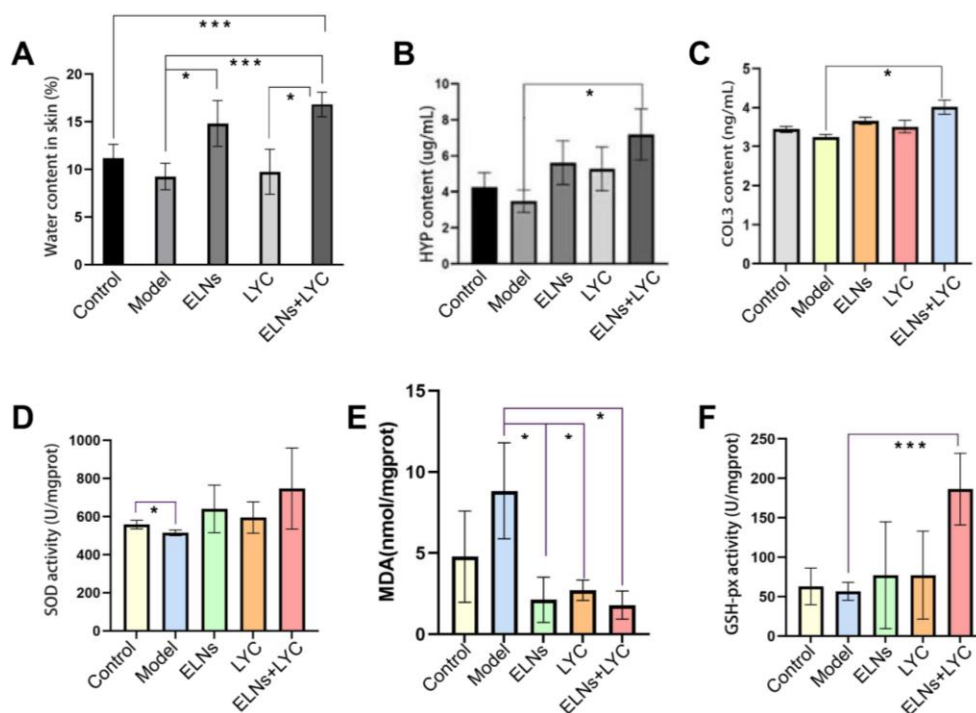


Figure 3. Biochemical analysis indexes of mice skins in different groups. **A.** Mice skin water content. **B.** HYP. **C.** Type III collagens. **D.** SOD. **E.** MDA. **F.** GSH-px. *: $P < 0.05$. ***: $P < 0.001$.

oxidative stress, ROS accumulate in skin cells, whereas SOD plays a critical role in scavenging superoxide anion radicals and is involved in inflammation, tumor progression, and autoimmune diseases [26]. In addition to its antioxidant properties, SOD also regulates cellular signaling and gene expression. The results showed that SOD activity in the normal group was significantly higher than that in the model group ($P < 0.05$) with the highest activity observed in the ELNs + LYC group (Figure 3D). Lipid peroxidation is a well-established mechanism of cellular damage, and MDA, a stable end-product of lipid peroxidation, can impair protein structure and function by forming adducts, serving as a key biomarker of oxidative stress [27]. The MDA content in the skin homogenates of the model group was significantly higher than that in the ELNs, LYC, and ELNs + LYC groups ($P < 0.05$) (Figure 3E). GSH-px levels were significantly increased in the ELNs + LYC group compared to that in the model group ($P < 0.001$), indicating an enhanced antioxidant defense (Figure 3F).

ELNs and LYC synergistically regulated the expression of aging-related genes

Type III collagen is an essential component of the extracellular matrix in the skin and is a form of elastic collagen. However, the content of type III collagen in the skin gradually declines with aging, leading to decreased skin elasticity and firmness along with the appearance of wrinkles and sagging skin [28]. Fibroblasts in the skin are responsible for the synthesis and secretion of type III collagen through complex signaling pathways and gene regulation mechanisms. Matrix metalloproteinases (MMPs), particularly MMP-1, are closely associated with type III collagen. MMP-1, a protease capable of degrading various extracellular matrix components, primarily targets type I and type III collagen [29]. In this research, the mRNA expression level of MMP-1 in mice skin tissues was significantly upregulated in the model group compared to the normal group ($P < 0.05$). Notably, the ELNs + LYC combination group showed a 42.7% reduction in MMP-1 transcriptional expression compared to the

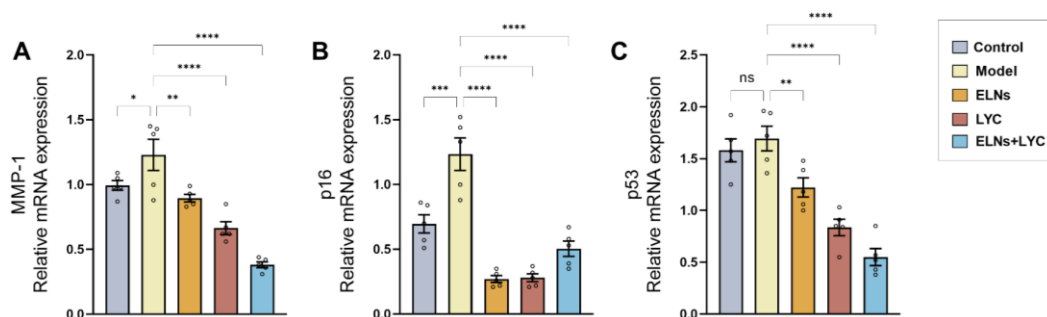


Figure 4. mRNA expression levels of aging-related genes in mice skins. **A.** MMP-1. **B.** p16. **C.** p53. ns: $P > 0.05$. *: $P < 0.05$. **: $P < 0.01$. ***: $P < 0.001$. ****: $P < 0.0001$.

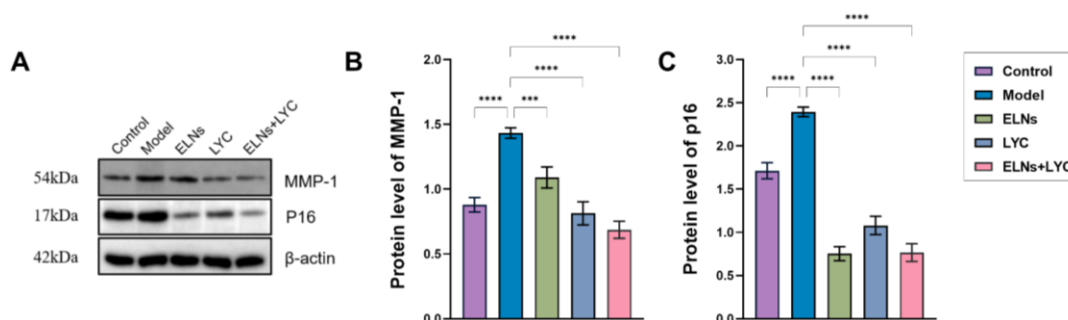


Figure 5. Protein expression level of skin aging-related genes in mice skins. **A.** Western blot image. **B.** MMP-1. **C.** p16. ***: $P < 0.001$. ****: $P < 0.0001$.

model group ($P < 0.0001$), indicating a synergistic inhibitory effect of the combined treatment on MMP-1 gene expression (Figure 4A). With advancing age, the expression level of P16 in skin increased, which may be associated with reduced cellular proliferation, cell cycle arrest, and cellular senescence during the aging process [30]. P16 exerts its effects by inhibiting the activity of cyclin-dependent kinases (CDKs), thereby inducing cell cycle arrest and suppressing cell proliferation. The upregulation of P16 expression may promote skin cell senescence and apoptosis, ultimately accelerating the skin aging process. The mRNA expression level of P16 in the model group was 3.2-fold higher than that in the normal group ($P < 0.001$) and the other treatment groups ($P < 0.001$). Notably, the ELNs + LYC combination group exhibited a 68% reduction in P16 expression relative to the model group, indicating a strong inhibitory effect on this aging-related gene (Figure 4B). P53 is a critical tumor suppressor gene that plays a key role in the regulation of the cell cycle, DNA repair, and

apoptosis, and it is closely associated with the aging process [31]. As aging progresses, the expression level of P53 tends to increase, leading to reduced cell proliferation, enhanced apoptosis, and impaired DNA damage repair capacity. There was no significant difference in P53 mRNA expression between the normal and model groups ($P > 0.05$). However, compared to the model group, the ELNs + LYC treatment group exhibited a 29% reduction in P53 mRNA expression ($P < 0.0001$), indicating that the combination intervention effectively suppressed P53 expression (Figure 4C). Western blot analyses of protein expression provided complementary evidence. Quantification of MMP-1 protein levels showed a 2.8-fold increase in the model group compared to normal control ($P < 0.001$), which was effectively normalized by ELNs + LYC treatment (58% reduction, $P < 0.001$) (Figure 5B). Similarly, P16 protein expression followed parallel trends with the model group exhibiting 3.1-fold higher levels than normal skin ($P < 0.001$), while ELNs + LYC administration

reduced P16 expression to near-baseline levels (72% suppression, $P < 0.001$) (Figure 5C). These molecular findings collectively demonstrated that the ELNs + LYC formulation significantly attenuated skin aging through dual inhibition of both MMP-1 and P16 pathways.

Conclusion

The combination of green tea-derived ELNs and lycopene exerted a protective effect against D-gal-induced aging in mice. The underlying anti-aging mechanism might involve enhanced antioxidant capacity through the elimination of excessive free radicals, inhibition of MMP-1, P16, and P53 expression, and reduced degradation of type III collagen. Therefore, this research recommended that it would be economically valuable to include them in the production of anti-skin-aging phytocosmetics.

Acknowledgements

This work was supported financially by the National Natural Science Foundation of China (Grant No. 31100499 and 31672394), the Key Research & Development Program of Zhejiang Province (Grant No. 2024C03075), and the Key Project of Science and Technology Plan of Zhejiang Provincial Market Supervision and Administration Bureau (Grant No. ZD2025026).

References

- Mine S, Fortunel NO, Pageon H, Asselineau D. 2008. Aging alters functionally human dermal papillary fibroblasts but not reticular fibroblasts: A new view of skin morphogenesis and aging. *PloS One*. 3(12):e4066.
- Conradt G, Hausser I, Nyström A. 2024. Epidermal or dermal collagen VII is sufficient for skin integrity: insights to anchoring fibril homeostasis. *J Invest Dermatol*. 144(6):1301-1310.
- Khan UM, Sevindik M, Zarrabi A, Nami M, Ozdemir B, Kaplan DN, et al. 2021. Lycopene: Food sources, biological activities, and human health benefits. *Oxid Med Cell Longevity*. 1:2713511.
- Kim JH, Yi YS, Kim MY, Cho JY. 2017. Role of ginsenosides, the main active components of Panax ginseng in inflammatory responses and diseases. *J Ginseng Res*. 41(4):435-443.
- Yang C, Zhang M, Lu S, Zhang T, Ma L, Meng X, et al. 2024. Compound enzyme treatment depolymerizes cell wall polysaccharides and improves pulp quality of *Goji Berry* (*Lycium barbarum* L.). *J Food Meas Charact*. 18(11):9252-9270.
- Zhao M, Yin Z, Ye H, Chen Q, Li F. 2020. Antioxidant mechanism of tea polyphenols and its impact on health benefits. *Anim Nutr*. 6(2):115-123.
- Zhang C, Song X, Cui W, Yang Q. 2021. Antioxidant and anti-ageing effects of enzymatic polysaccharide from *Pleurotus eryngii* residue. *Int J Biol Macromol*. 173:341-350.
- Liu P, Chen G, Zhang J. 2022. A review of liposomes as a drug delivery system: Current status of approved products, regulatory environments, and future perspectives. *Molecules*. 27(4):1372.
- Alshawwa SZ, Kassem AA, Farid RM, Mostafa SK, Labib GS. 2022. Nanocarrier drug delivery systems: characterization, limitations, future perspectives and implementation of artificial intelligence. *Pharmaceutics*. 14(4):883.
- Du S, Guan Y, Xie A, Yan Z, Gao S, Li W, et al. 2023. Extracellular vesicles: A rising star for therapeutics and drug delivery. *J Nanobiotechnol*. 21(1):231.
- Liu BL, Yu H, Shi X, Zhou Y, Alvarez S, Yu J, et al. 2021. Therapeutic potential of garlic chive-derived vesicle-like nanoparticles in NLRP3 inflammasome-mediated inflammatory diseases. *Theranostics*. 11(19):9311-9330.
- Zhang MZ, Viennois E, Prasad M, Zhang YC, Wang LX, Zhang Z, et al. 2016. Edible ginger-derived nanoparticles: A novel therapeutic approach for the prevention and treatment of inflammatory bowel disease and colitis-associated cancer. *Biomaterials*. 101:321-340.
- Bai C, Zhang X, Li Y, Qin Q, Song H, Yuan C, et al. 2024. Research status and challenges of plant-derived exosome-like nanoparticles. *Biomed Pharmacother*. 174:116543.
- Kim JS, Lee HJ, Yoon EJ, Lee H, Ji Y, Kim Y, et al. 2023. Protective effect of *Iris germanica* L. Rhizome-derived exosome against oxidative-stress-induced cellular senescence in human epidermal keratinocytes. *Appl Sci*. 13(21):11681.
- Fei T, Fei J, Huang F, Xie T, Xu J, Zhou Y, et al. 2017. The anti-aging and anti-oxidation effects of tea water extract in *Caenorhabditis elegans*. *Exp Gerontol*. 97:89-96.
- Ke J, Li J, Yang Z, Wu H, Yu J, Yang Y, et al. 2024. Unraveling anti-aging mystery of green tea in *C. elegans*: Chemical truth and multiple mechanisms. *Food Chem*. 460:140510.
- Cheng M, Song J, Lei X, Li H, Chen S, Zhao J, et al. 2024. Study on the delaying effect of green tea exosome like nanoparticles (ELNs) on the aging of human fibroblasts. *J Tea Commun*. 51(3):391-400.
- Zu M, Xie D, Canup BSB, Chen N, Wang Y, Sun R, et al. 2021. 'Green' nanotherapeutics from tea leaves for orally targeted prevention and alleviation of colon diseases. *Biomaterials*. 279:121178.
- Pan LS, Wang WC, Yao MY, Zhang XZ. 2023. Research progress on plant-derived exosome-like nanoparticles and their applications. *J Chin Mater Med*. 48(22):5977-5984.

20. Göncü T, Oğuz E, Sezen H, Koçarslan S, Oğuz H, Akal A, *et al.* 2016. Anti-inflammatory effect of lycopene on endotoxin-induced uveitis in rats. *Arq Bras Oftalmol.* 79:357-362.
21. Shen L, Fan L, Zhang Y, Shen Y, Su Z, Peng G, *et al.* 2022. Antioxidant capacity and protective effect of cow placenta extract on d-galactose-induced skin aging in mice. *Nutrients.* 14(21):4659.
22. Anusha R, Priya S. 2022. Dietary exosome -like nanoparticles: An updated review on their pharmacological and drug delivery applications. *Mol Nutr Food Res.* 66(14):2200142.
23. Srivastava AK, Khare P, Nagar HK, Raghuvanshi N, Srivastava R. 2016. Hydroxyproline: A potential biochemical marker and its role in the pathogenesis of different diseases. *Curr Protein Pept Sci.* 17(6):596-602.
24. Hua C, Zhu Y, Xu W, Ye S, Zhang R, Lu L, *et al.* 2019. Characterization by high-resolution crystal structure analysis of a triple-helix region of human collagen type III with potent cell adhesion activity. *Biochem Biophys Res Commun.* 508(4):1018-1023.
25. Gu Y, Han J, Jiang C, Zhang Y. 2020. Biomarkers, oxidative stress and autophagy in skin aging. *Ageing Res Rev.* 59:101036.
26. Younus H. 2018. Therapeutic potentials of superoxide dismutase. *Int J Health Sci.* 12(3):88.
27. Su D, Wang X, Zhang W, Li P, Tang B. 2022. Fluorescence imaging for visualizing the bioactive molecules of lipid peroxidation within biological systems. *Trend Anal Chem.* 146:116484.
28. Lovell CR, Smolenski KA, Duance VC, Light ND, Young S, Dyson M. 1987. Type I and III collagen content and fibre distribution in normal human skin during ageing. *Br J Dermatol.* 117(4):419-428.
29. Murphy G, Nagase H. 2008. Progress in matrix metalloproteinase research. *Mol Aspects Med.* 29(5):290-308.
30. Majewska J, Agrawal A, Mayo A, Roitman L, Chatterjee R, Sekeresova KJ, *et al.* 2024. p16-dependent increase of PD-L1 stability regulates immunosurveillance of senescent cells. *Nat Cell Biol.* 26(8):1336-1345.
31. Mijit M, Caracciolo V, Melillo A, Amicarelli F, Giordano A. 2020. Role of p53 in the regulation of cellular senescence. *Biomolecules.* 10(3):420.